



UNIVERSITÀ POLITECNICA DELLE MARCHE  
Repository ISTITUZIONALE

Advanced numerical analyses by the Non-Smooth Contact Dynamics method of an ancient masonry bell tower

This is the peer reviewed version of the following article:

*Original*

Advanced numerical analyses by the Non-Smooth Contact Dynamics method of an ancient masonry bell tower / Ferrante, A.; Clementi, F.; Milani, G.. - In: MATHEMATICAL METHODS IN THE APPLIED SCIENCES. - ISSN 0170-4214. - STAMPA. - 43:12(2020), pp. 7706-7725. [10.1002/mma.6113]

*Availability:*

This version is available at: 11566/273439 since: 2024-04-28T12:42:51Z

*Publisher:*

*Published*

DOI:10.1002/mma.6113

*Terms of use:*

The terms and conditions for the reuse of this version of the manuscript are specified in the publishing policy. The use of copyrighted works requires the consent of the rights' holder (author or publisher). Works made available under a Creative Commons license or a Publisher's custom-made license can be used according to the terms and conditions contained therein. See editor's website for further information and terms and conditions.

This item was downloaded from IRIS Università Politecnica delle Marche (<https://iris.univpm.it>). When citing, please refer to the published version.

(Article begins on next page)

# Advanced numerical analyses by the Non-Smooth Contact Dynamics method of an ancient masonry bell tower

*<sup>1</sup>Angela Ferrante, <sup>1</sup>Francesco Clementi, <sup>2</sup>Gabriele Milani\**

*<sup>1</sup>Department of Civil and Building Engineering, and Architecture, Polytechnic University of Marche, via Breccie Bianche, 60131, Ancona, Italy*

*<sup>2</sup>Department of Architecture, Built Environment and Construction Engineering ABC, Polytechnic of Milano, Piazza Leonardo da Vinci 32, 20133, Milan, Italy*

*\*Corresponding author: [gabriele.milani@polimi.it](mailto:gabriele.milani@polimi.it)*

**Keywords:** Discrete Element Method, Masonry Tower, Non-Smooth Contact Dynamics method, Nonlinear Dynamic Analysis

**Abstract:** Advanced numerical analyses were carried out in order to assess the nonlinear dynamical behaviour of the bell tower of Pomposa Abbey in Codigoro, in the province of Ferrara (Italy), by means of the Non-Smooth Contact Dynamics (NSCD) method. The main purpose of the work is to investigate the capacity of the main mechanical parameter used in the analysis, namely the friction coefficient, to have effects on the mechanical response of ancient masonry structures undergoing seismic actions. Therefore, the tower was modelled following the Discrete Element Method (DEM) and assembling the masonry texture as rigid bodies tied by frictional joints. Thus, a discontinuous approach was used to assess the dynamic properties and the vulnerability of the masonry structure, through large deformations regulated by the Signorini's law, concerning the impenetrability between the rigid bodies, and by the Coulomb's law, regarding the dry-friction model. Afterward, different values were assigned to the friction coefficient of the models and a variety of real seismic shocks have been applied in the nonlinear analyses. Finally, it is possible to see different failure mechanisms resulting for each friction value and types of dynamic actions used, as expected.

## 1. Introduction

The damage assessment of historical masonry buildings is one of the most difficult tasks to be investigated in structural mechanics, since this kind of structures is commonly heterogeneous, with complex geometries, irregularities and absence of a box behaviour due to defective connections between different structural parts, in particular walls and floors, that often play a fundamental role. However, the knowledge of the dynamical behaviour is crucial for a reliable seismic vulnerability assessment, which became more and more important due to the recent catastrophic earthquakes that stroked Italy in the last few decades (Umbria-Marche 1997–1998, Abruzzo 2009, Emilia-Romagna 2012, Marche-Lazio-Umbria-Abruzzo 2016) [1–4].

Masonry towers and belfries are part of a peculiar structural type which characterizes the Italian architectural heritage, such as the civic clock towers in the ancient cities' centres, the bell towers of churches and defence structures of the medieval fortresses. All these structures are distinguished by the poor-quality local materials by which they were often constituted, i.e. mostly unplastered and bound by poor mortar brick masonry walls. Furthermore, these buildings are based on simple architectural forms, with a predominant vertical development. Hence, even though they may exhibit different geometries in terms of slenderness, base shear area, perforations, wall thicknesses and internal irregularities, they are built with similar technologies and made of masonries having similar mechanical properties. For these reasons, the primary aim is to develop a detailed analysis of interpretative models that can efficaciously predict the behaviour of these structures under seismic actions [5–12]. Another key issue is the effect induced by the application of vertical accelerograms on the structural behaviour of high structures that may be quite relevant in some cases, thus it is necessary to use a set of vertical and horizontal time-history acceleration for the models.

To investigate the mechanical behaviour of masonry structures, commonly Finite Element Methods (FEM) are utilized, often including very sophisticated constitutive laws taking into account post-elastic behaviours and damage, and they have a wide range of application reported in the technical literature [13–18]. These methods, while being very appealing, do not focus on the possible non-smooth nature of the dynamic response, which can come sliding and impacting between different blocks, and situation that is common just before and during the collapse [19–25].

Moreover, the ancient masonry structures may be seen as discontinuous structural systems composed of units (e.g. bricks, stones, blocks, etc.), bonded together with or without mortar. Thus, to gain a numerical model able to adequately represent the behaviour of a real structure, both the constitutive model and the input material properties must be selected carefully by the modeler to take into account the variation of masonry properties and the range of stress state types that exist in masonry structures [13,15,26–33].

For this reason, the dynamics of ancient masonry structures is numerically investigated in this study by means of the Non-Smooth Contact Dynamics method (NSCD) which is implemented on a distinct element code [34–37], namely LMGC90©, and the progress in parallel-processing technology made this approach viable for increasingly large systems, compared to the past [38,39].

In particular, the NSCD method was applied on advanced numerical models to survey the dynamical behaviour of the ancient masonry bell tower subject to strong non-linear

dynamic actions and the modalities of progressive collapse mechanisms. Consequently, these characteristic masonry structures inside the epicentral area of the North-East Italy shocks of May 2012 were discretized in very detailed 3D models. These models were achieved through rigid blocks bounded together by points of contacts, which follow the Signorini's law, about the impenetrability condition, and the Coulomb's law, relative to dry-friction [40]. Thus, this approach pointed out discontinuous nonlinear dynamics of the structures, allowing to explore it. In fact, the main appeal of this approach lies in its capabilities to reproduce complex behaviour, as complete block separation and large movements, with substantial changes in the whole structure.

Finally, the masonry structure studied in this paper is the bell tower belongs to Pomposa monastery complex in the municipality of Codigoro, in the province of Ferrara in Italy, as in Figure 1. A dynamic identification [5,41–45] with a calibration of a first numerical (continuum) model was also carried out in 2016 [46]. Actually, the present work aims to investigate the influence of the main mechanical parameters used in the NSCD method, namely the friction coefficient, on the dynamical behaviour of the vertical structure under the action of the six different sets of ground accelerations related to most recent Italian earthquakes.

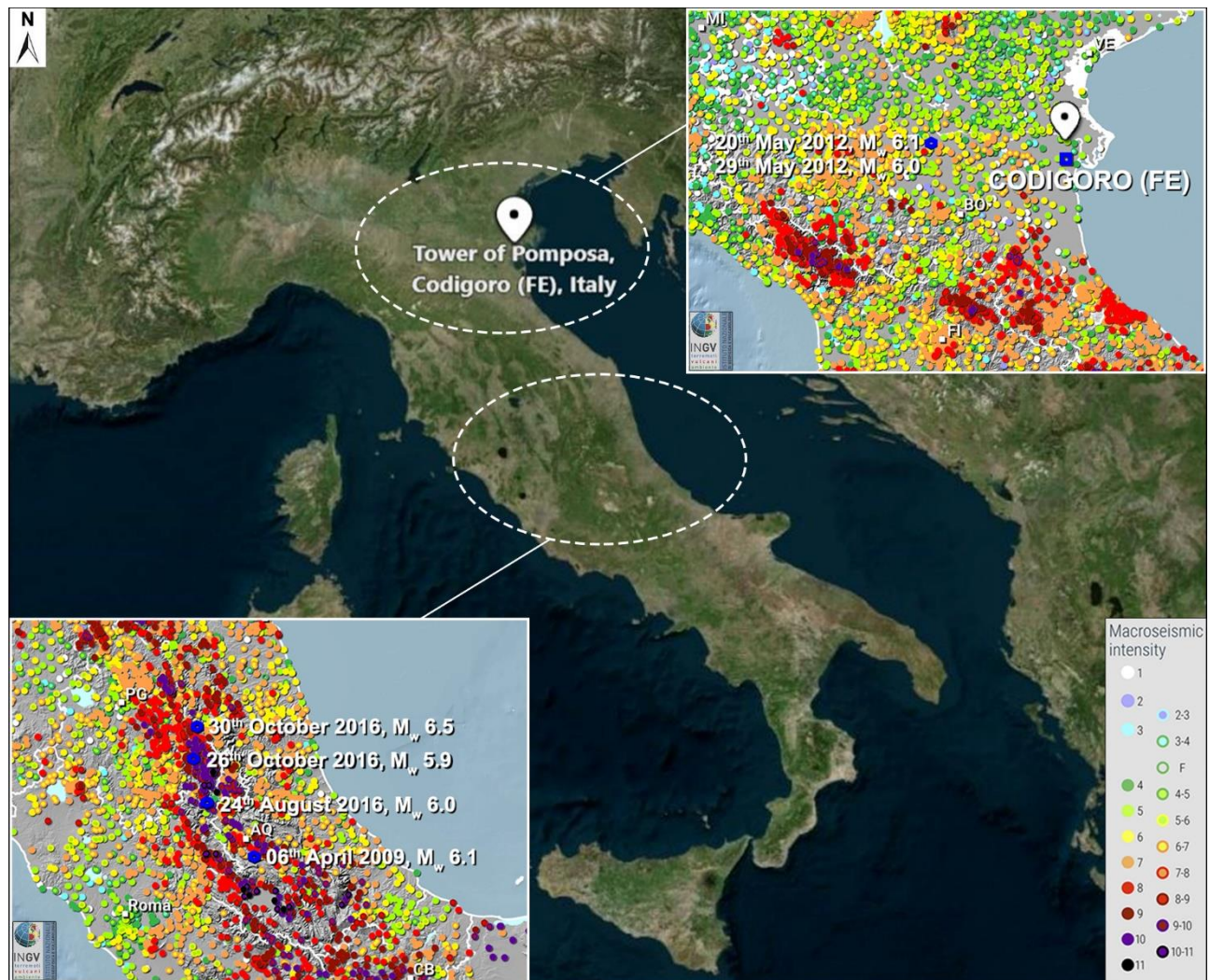


Figure 1\_Geographical location of the bell tower of Pomposa in Codigoro (Ferrara, Italy) and of the epicentres of the six main seismic events of the last few decades in Italy on the Italian Macroseismic intensity map (<https://emidius.mi.ingv.it/>)



## 2. Architectural description of Pomposa tower

A masterpiece of Romanesque art, the Pomposa monastery complex is located in Codigoro, in the province of Ferrara in Italy, and it is situated within the park of the Po Delta, constituting a historical - architectural and religious component of great value, accessible by the Provincial road that was the Ancient pilgrims' way of Middle Ages.

The abbey of Pomposa has a few historical information that accurately documents its foundation. The presence of Pomposa is certain to be existing in the VI-VII century and it is formally cited for the first time in a document of 874, while under the protection of Ravenna, it is mentioned in the Fragment of a letter that Pope John VIII sent to Emperor Ludwig II. The Pomposa island, geographically defined until the XII century by two main branches of the Po's river, promoted the development of a rich and powerful monastery, which reaches the peak of its fame and independence in the XI century.

Afterward, in 1026 the church was re-consecrated, and it became a primary centre of religious and spiritual life for the region. In 1063 the bell tower was built by the Magister Deusdedit and, in the same year, the Cloister saw the light. Later, in the XVI century, Pomposa was in strong decline: the site became marshy and malaric and it no longer allowed the presence of the community. Then, in 1423 the abbey was assigned among the assets of the new monastery of San Benedetto in Ferrara and in 1653 the Pope Innocent X formally decreed the suppression of the Pomposa cenoby from which the last monks came out in 1671. Finally, in 1802 the buildings were annexed to the agricultural estate, that the Guiccioli bought and used as warehouses, stables, barns, until the 1900s, when they were redeemed with the restitution to the State followed by large restorations.



(a)



(c)



(b)



(d)

Figure 2\_ Views of the abbey (a, b) and of the bell tower (c, d) of Pomposa in Codigoro (Ferrara, Italy)

The Pomposa Abbey is a typical Benedictine monastery, as visible in Figure 2 (a, b), where the bell tower arises near the church Figure 2 (c, d).

The ancient tower is a wonderful example of Romanesque architecture and a symbol of the Benedictine economic and cultural power. It is accessible to the public from the outside, with the entrance located both on the east side and on the south side, inside the abbey. In this study, it was conceived as an isolated building and the connection between the abbey and the tower was not considered since the two arose in different eras and they are not structurally connected. Over the years, the bell tower did not undergo significant alterations, just numerous minor interventions. The first restoration dates back to 1879 when the upper cone was partially rebuilt following a collapse due to lightning; in that occasion, the walls were secured, and chains were inserted at the level of the floors. In 1920 the mullioned arches were almost completely reopened. In recent years, the University of Ferrara began an investigation aimed at verifying the structural condition of the church, that has strongly distorted walls and large cracks due to the presence of the bell tower. In fact, the weight of the tower, about 1800 tons, caused his yielding with consequent dragging and inclination of it and a good part of the elevated structures of the church. Furthermore, the earthquakes that struck the Emilia-Romagna region in 2012 did not cause damages to the abbey and the bell tower.

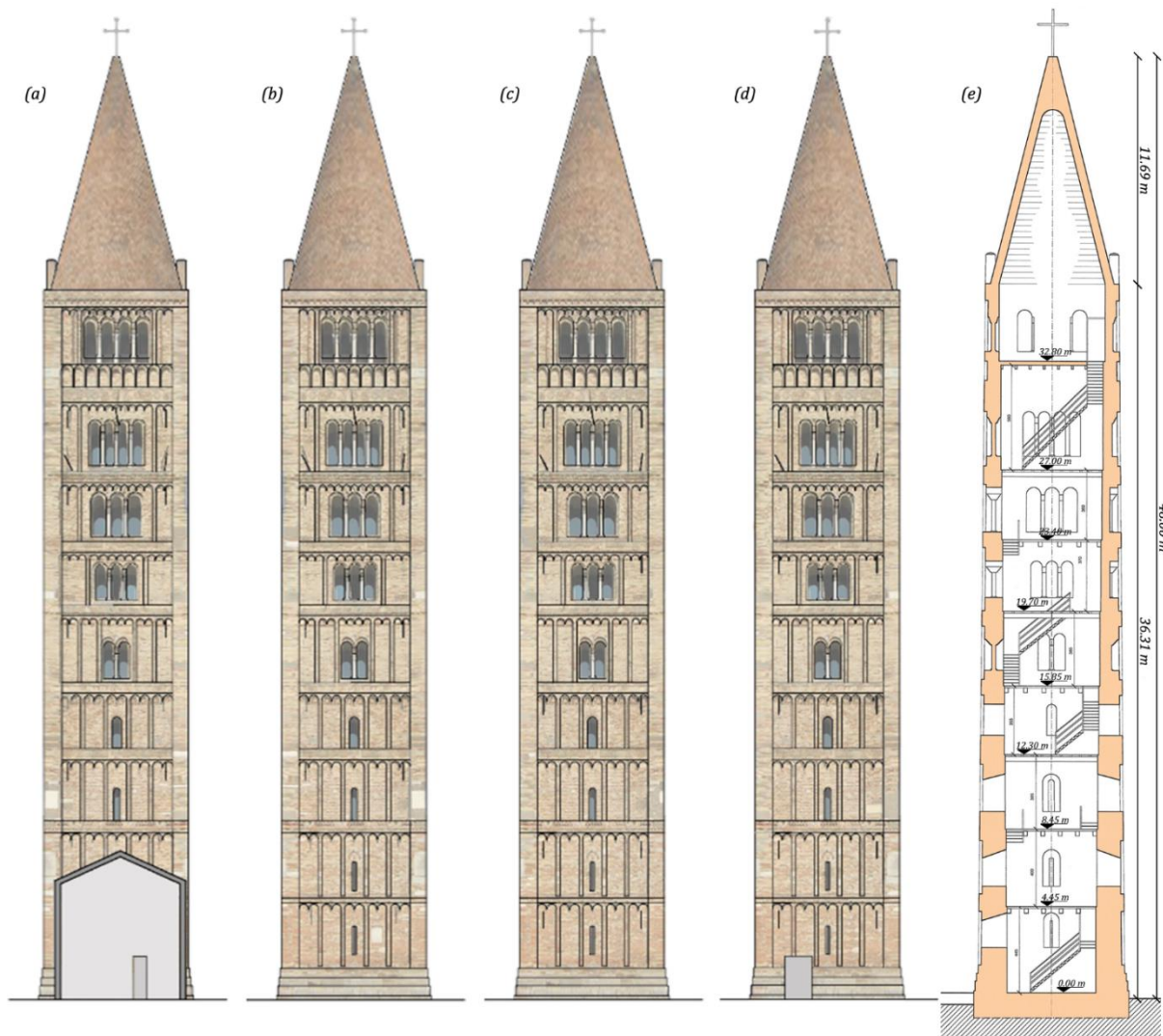


Figure 3\_ Drawings of the bell tower of Pomposa Abbey in Codigoro (Italy): South-West façade (a), North-West façade (b), North-East façade (c), South-East façade (d) and vertical cross section (e)

The tower is 48.00 m high and has a square plant, with long sides of 7.60 x 7.60 m at the base, that decrease along with the height, as visible in Figure 3. It consists of nine modules, plotted in Figure 4, culminating on the top by a conical dome. By placing the reference at the level of the ground floor, the plans are: ground floor (P0) at 0.00 m, first floor (P1) at 4.45 m, second floor (P2) at 8.45 m, third floor (P3) at 12.30 m, fourth floor (P4) at 15.85 m, fifth floor (P5) at 19.70 m, sixth floor (P6) at 23.40 m, seventh floor (P7) at 27.00 m and floor of the cell bell (P8) at 32.80 m.

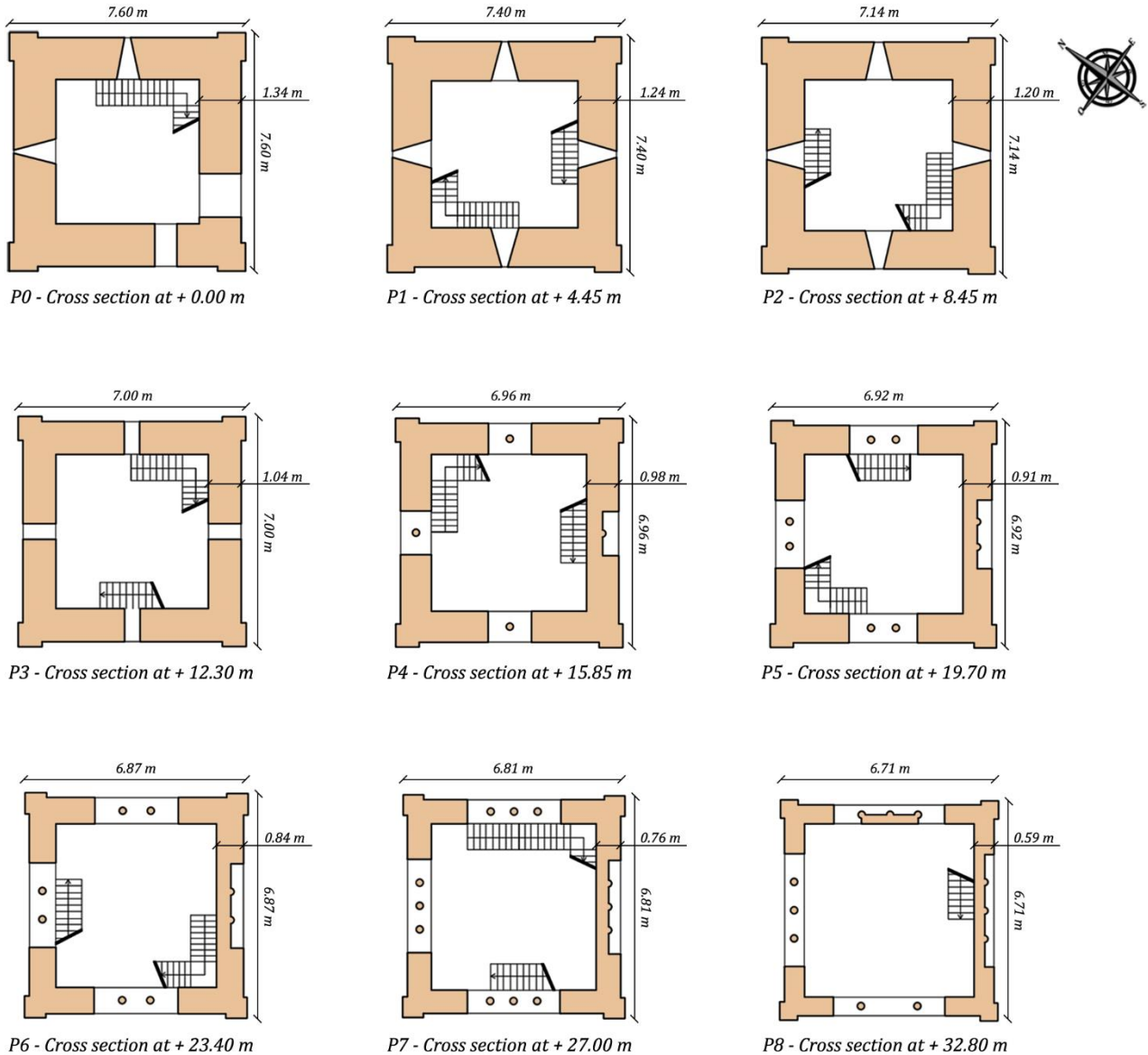


Figure 4\_ Drawings of the cross sections of the bell tower of Pomposa Abbey in Codigoro (Italy)

This ancient tower is built on a truncated pyramid shape base of dimensions about 8.02 x 8.02 x 1.64 m, which is made by marble blocks of reuse, as visible in Figure 5 (c). Moreover, every façade is contained by two lateral pilasters and is richly decorated by hanging arches and designs obtained by using bricks of different shades. The external façade in red and yellow bricks preserves very rare marble fragments of re-use (18 ancient ones, the others from the modern era): they date back to the XI century and they come from various Mediterranean countries, such as Egypt, Tunisia, and Sicily. The internal walls are not plastered and, therefore, the texture of the masonry is visible. The vertical structure is characterized by thick brick walls



ranging from 0.59 m to 1.34 m. The mass of the tower is lightened upwards by a series of windows, splayed and aligned, gradually increasing in number and width in order to lighten the weight of the construction: from the thin single-light window on the first floor you reach the four-light arched windows in the upper part. In particular, the first two modules have rectangular windows of 0.21 x 1.41 m, the third and fourth modules have single arched windows with dimensions of 1.40 x 1.70 m, the fifth has mullioned windows of 2.19 x 1.92 m, the sixth and seventh have three-light windows of 2.69 x 2.2 m and, lastly, the eighth and ninth have four-light windows of 3.56 x 2.08 m, as in Figure 5 (a). The columns of the arched windows are of marble with a diameter of 0.3 m (see Figure 5 (b)).



(a)



(b)



(c)



(d)

*Figure 5\_ Views of the arched openings (a) and their columns (b); photo of the basement (c) and a particular of the P8 floor (d) of the Pomposa tower in Codigoro (Ferrara, Italy)*

Regarding the connections between the transversal walls, some chains were inserted. Two chains in particular were introduced in the north-south direction at floor P1, P2, P4, P6, P7, P8 and in the east-west direction at floor P3, P5, P7, P8.

The final floors are all made of wood, with orthogonal framework to prevent overloading the masonry walls, except at P8 where there is a one-way RC ribbed-slab. The wooden floors



are made by square beams of 0.30 x 0.30 m arranged in a wheelbase of 1.1 m, secondary beams of 0.06 x 0.06 m at intervals of 0.30 m and planks with thick of 0.03 m. The RC ribbed-slab consists of a slab with a 0.06 m thickness and precast beams, namely Varese, see Figure 5 (d), with thick of 0.16 m with interaxis of 0.8 m. The vertical connection consists of wooden stairs, which were not modelled but considered in terms of inertial masses. The coverage of the tower has a conical shape with dimensions of 6.35 x 11.69 m.

### 3. Distinct element method for historical masonry

Ancient masonry structures exhibit complex behaviours, due to the heterogeneity and irregularities of their elements and the various material properties composing them. Hence, for the conservation of the cultural heritage, rich of historical masonry, an accurate modelling and an exhaustive assessment of these existing structures becomes crucial.

For this reason, the numerical analyses of masonry buildings are widespread and numerous, according to different approaches. In fact, the most used is macro-modelling, i.e. continuum medium, which takes homogenisation technique into account. However, to recreate the real geometry, with the interaction between distinct blocks, the use of simplified micro-models [47–49] is more appropriate, like the Non-Smooth Contact Dynamics Method (NSCD). In fact, this method permits to assess the dynamic global behaviour of the masonry through the local behaviour. Moreover, the interfaces between blocks contains the contact points that allow to have frictional behaviour of joints, which are regulated by the Coulomb's law and Signorini's impenetrability.

Hence, to apply this discrete modelling, the LMGC90<sup>©</sup> open source software was used in this work, which implements the Non-Smooth Contact Dynamics method, with implicit time integration and contact solvers.

#### 3.1 NSCD for masonry structures modelling

The discrete modelling permits to describe the masonry as the interaction between blocks and it assumed that the properties of the bodies and their contact points govern the model. Moreover, for simplifying, the contact is supposed to be punctual and not an area of the interfaces. Other relevant hypotheses assumed in this method are that the bodies are rigid, with the strain applied to the contact points, and the contact forces are provided by the strain at the punctual contact, with independent interactions between bodies.

The approach of the Non-Smooth Contact Dynamics involves first the contact detection, then the contact problem, i.e. the derivation of the contact forces for local scale, and last the individuation of bodies displacement, for global scale. In fact, in the framework of the NSCD, to compute the multi-contact problem it is necessary the resolution of the local unknowns, due to the interactions, and the global unknowns, due to the bodies. These two sets of unknowns are bounding by a mapping (see Figure 6).

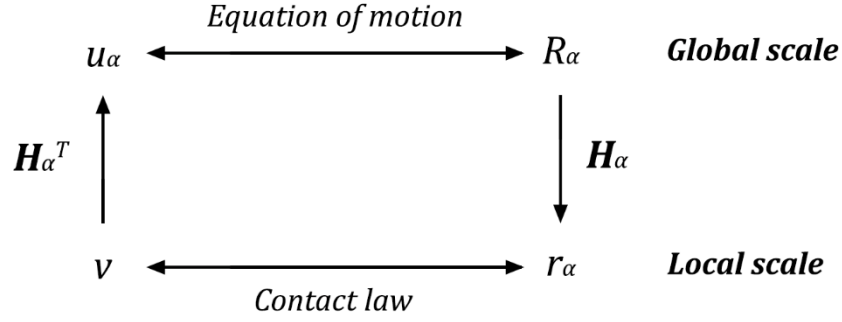


Figure 6\_ Global and local mapping in the NSCD algorithm

At the contact  $\alpha$ , a linear mapping  $\mathbf{H}_\alpha$  allow to obtain the global resultant forces  $R_\alpha$  related to the local forces  $r_\alpha$ , with the equation:

$$R_\alpha = \mathbf{H}_\alpha(q)r_\alpha . \quad (1)$$

$\mathbf{H}_\alpha(q)$  is a mapping with the local information of the contactors and  $q$  is the vector of generalised coordinates of the rigid displacement. Hence, to achieve the global resultant contact forces exerted on bodies:

$$R = \sum_\alpha R_\alpha . \quad (2)$$

Moreover, to calculate the velocity  $u_\alpha$  relative to contact in relation with the velocity of the blocks, it can be used the transposed  $\mathbf{H}^T$  as in this equation:

$$u_\alpha = \mathbf{H}^T(q)v , \quad (3)$$

with  $v$  is the time derivative of  $q$ .

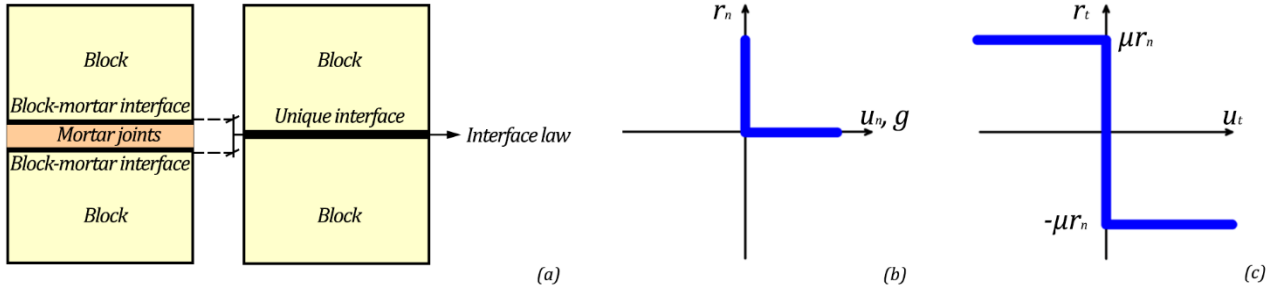


Figure 7\_ Contact at the interface between blocks (a), Signorini's impenetrability condition (b), and friction Coulomb's law (c)

The reaction force and the relative velocity of the contact are described by the laws of Signorini and Coulomb. In fact, the impenetrability of contact between blocks is represented by the Signorini's condition (see Figure 7 (b)), written as:

$$\begin{cases} g \geq 0 , \\ r_n \geq 0 , \\ g \cdot r_n = 0 , \end{cases} \quad (4)$$

where  $g$  is the distance between the bodies and  $r_n$  is the normal component of the contact force. The same equations can be written for the velocities, considering the normal component  $u_n$  , in the following way:

$$\begin{cases} g(t_0) \geq 0 \text{ at initial time step } t_0, \\ g(t) \leq 0 \Rightarrow u_n \geq 0, r_n \geq 0, u_n r_n = 0. \end{cases} \quad (5)$$

Additionally, the dry friction Coulomb's law (see Figure 7 (c)) permits to comprehend the tangential force between blocks and the sliding, as written in the following system:

$$\begin{cases} \|u_T\| = 0, \|r_T\| < \mu r_n \Rightarrow \|u_T\| = 0 & \text{Sticking,} \\ \|r_T\| = \mu r_n \Rightarrow u_T = -k r_T, k \geq 0, \|u_T\| \neq 0 & \text{Sliding,} \end{cases} \quad (6)$$

where  $\mu$  is the friction coefficient.

Thus, the bodies exhibit dynamics regulated by the following equation of motion:

$$\mathbf{M}(q)dv = F(q, v, t)dt + dI, \quad (7)$$

where  $\mathbf{M}$  is the mass matrix,  $F(q, v, t)$  is the vector of internal and external forces of the system,  $dt$  is the Lebesgue measure on  $\mathbb{R}$ ,  $dv$  is a differential measure of velocity denoting the acceleration measure and  $dI$  is a differential measure of the impulse of contact resultant.

It is important to highlight that it is not necessary to manage explicitly the contact events in the time-stepping integration scheme, as in the case of the event-driven scheme. The time subdivision is done on intervals  $[t_i, t_{i+1}]$  of length  $h$  and it is fixed, consequently it is possible to deal with a great number of discontinuities during one-time step, and the contact problem is solved over the range in terms of measures of this interval and not in a point-wise way. Thus, the Eq. (7) can be integrated on each time step, which involves to:

$$\mathbf{M}(v_{i+1} - v_i) = \int_{t_1}^{t_{i+1}} F(q, v, t)dt + I_{i+1}, \quad (8)$$

with the velocity  $v_{i+1}$  is the approximation of the right limit at the time  $t_{i+1}$ ,

$$\begin{cases} v_{i+1} = v_i + \mathbf{M}^{-1} \int_{t_1}^{t_{i+1}} F(q, v, t)dt + \mathbf{M}^{-1} I_{i+1}, \\ v_{free} = v_i + \mathbf{M}^{-1} \int_{t_1}^{t_{i+1}} F(q, v, t)dt, \end{cases} \quad (9)$$

where  $v_{free}$  is the velocity of the bodies in the absence of contacts. Hence, (9) can be rewritten by means of the Delassus operator  $\mathbf{W}^{\alpha\beta}$  and the local unknowns in this form:

$$\begin{cases} v_{i+1}^\alpha = v_{loc,free}^\alpha + \mathbf{W}^{\alpha\beta} I^\alpha, \\ \text{Contact law } (I^\alpha, v^\alpha) = 0, \end{cases} \quad (10)$$

and  $v_{loc,free}^\alpha = \mathbf{H}^{T\alpha}(q_m)v_{free} + \sum_{\beta \neq \alpha} \mathbf{W}^{\alpha\beta} I^\beta$ . Finally, the Non-Linear Gauss Seidel method allows to solve the contact problem.

Therefore, between the discrete element methods, there is the NSCD method, which is characterized by three main points: (i) the non-smooth contact laws are directly integrated inside it, (ii) an implicit integration scheme is implemented and (iii) structural damping are not considered into it. Furthermore, the NSCD method requires some simplifications on the building of models. First of all, the bodies are assumed perfectly rigid and, secondly, the contact laws between blocks are determined by the Signorini's impenetrability condition and by the dry-friction of Coulomb. Thus, these relations on the contacts involve the perfectly plastic impacts, hence without bounces as a consequence, i.e., a null value of the restitution coefficient in the Newton law. According to it, there is the main advantage of the limited computational



complexity derived by the simple modelling of the impacts. Afterward, another relevant benefit due to the perfectly plastic impact is related to the dissipation of energy, which explains the damages of the material and the micro-cracks of the stones after the collisions and, additionally, supports the numerical integration and its stability from a computational point of view. Actually, in these models, the dissipated energy is determined by the involvement of the friction and it does not consider the damping effects, which instead are essential for the continuum models.

#### 4. The bell tower's numerical model

The modelling of the Pomposa bell tower aims to obtain a geometry by means of the discontinuous approach and assigning appropriate mechanical properties to the model, thus to appreciate all the possible dynamical behaviour of the masonry under the influence of the friction coefficient between the blocks.

For this reason, the existing configuration of the tower was taken into account, with its actual dimensions and the past interventions still present on the masonry structure [50–53]. Moreover, the masonry panels were modeled while the wooden floor and the chains were not, the one-way RC ribbed-slabs and the conical dome were recreated as near to reality as possible. Thus the numerical model, as visible in Figure 8, is formed by 2031 rigid blocks of different dimensions and regular convex shapes. Otherwise, the mortar dimension is modeled as well as the bricks into the rigid blocks, assuming the null value of the joints. For what concerns other parameters, the mass density is related to the existing masonry, and it assumes specific values as indicated in the [54].

To study the influence of the friction on the structural behaviour, the values of the parameter should take into account the degradation of the mechanical characteristics over time [55]. Hence, for all the blocks along the elevation, values equal to  $\mu = 0.3$  were chosen to simulate a very poor kind of mortar, to  $\mu = 0.5$ , for quite good quality, and to  $\mu = 0.7$ , for a better type of it or renovated masonry walls. However, a value equal to  $\mu = 0.9$  was assigned considering the relationship between structure and foundation.

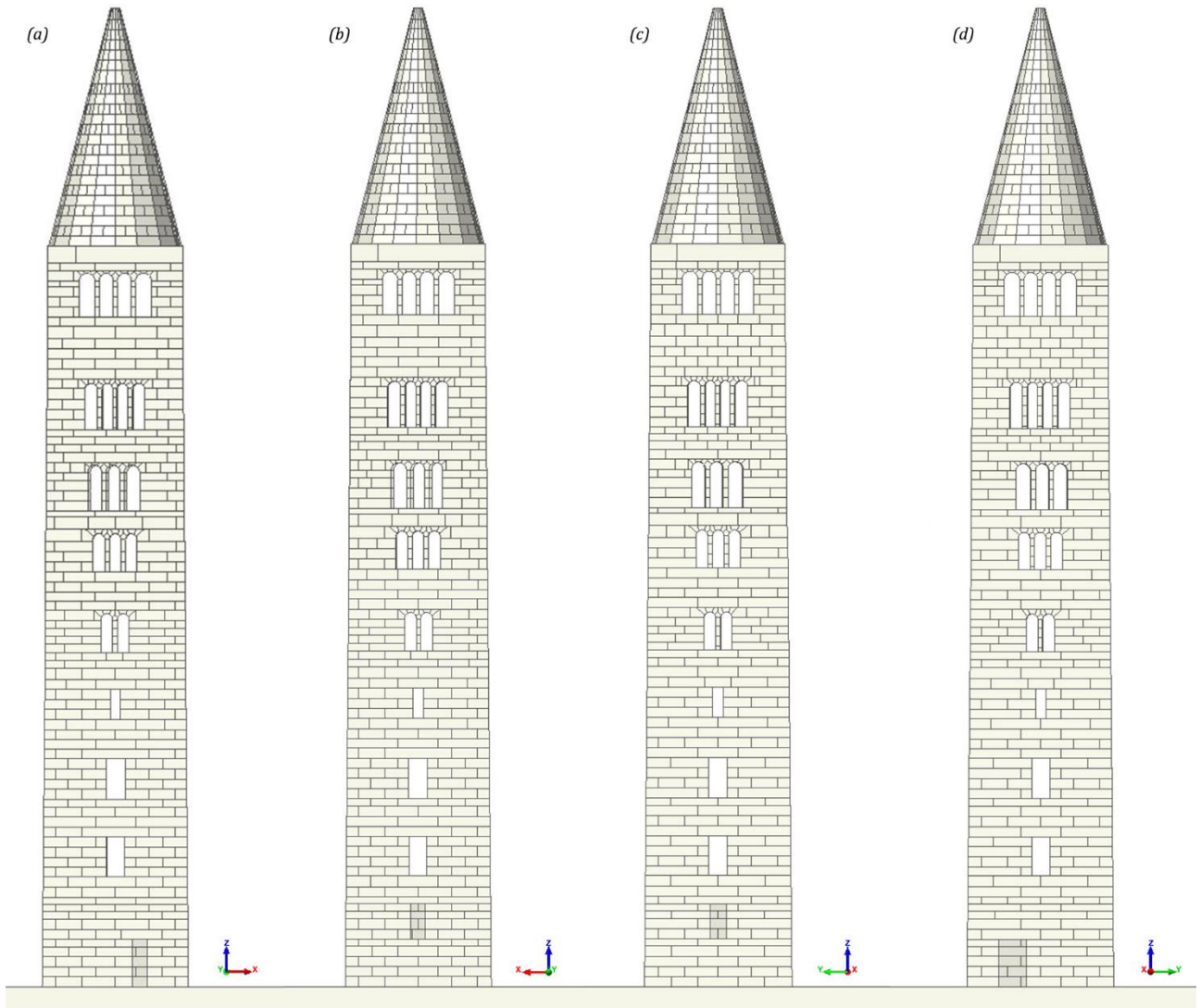


Figure 8\_ Views of the South-West façade (a), North-West façade (b), North-East façade (c), South-East façade (d) of the numerical models of the bell tower of Pomposa Abbey in Codigoro (Italy) with the NSCD method

Several analyses were implemented applying to the system first the gravity loads and afterward the different ground accelerations: the dynamic behavior was elaborated on shocks action of real events imported on the main directions of the base of the tower. The main shocks considered had various specifications; all of these are obtained by the records of seismic events occurred in the Italian territory. In particular, the recordings of velocities were taken by the stations of the epicenters, and in this paper, all three components, i.e. two on horizontal x and y and one on vertical z directions, are used. We considered two shock events of a sequence of 2012 that took place in North-East of Italy, near Ferrara where the analyzed tower is located, and further four earthquakes of the highly active seismological area of Central Italy, which belong to separate seismic sequences of 2009 and 2016:

- (i) 06<sup>th</sup> April 2009 L'Aquila with  $M_L=5.9$  and  $M_W=6.1$  (AQV station in Italian Accelerometric Archive (ITACA)),
- (ii) 20<sup>th</sup> May 2012 Mirandola with  $M_L=5.9$  and  $M_W=6.1$  (MRN station in ITACA),
- (iii) 29<sup>th</sup> May 2012 Mirandola with  $M_L=5.8$  and  $M_W=6.0$  (MRN station in ITACA),
- (iv) 24<sup>th</sup> August 2016 Amatrice with  $M_L=6.0$  and  $M_W=6.0$  (AMT station in ITACA),
- (v) 26<sup>th</sup> October 2016 Campi with  $M_L=5.9$  and  $M_W=5.9$  (CMI station in ITACA),

(vi) 30<sup>th</sup> October 2016 Forca Canapine  $M_L=6.1$  and  $M_W=6.5$  (FCC in ITACA).

The location of epicenters are plotted in Figure 1, and the comparison between the characteristics of the seismic accelerations is reported in Table 1, where [56–58]:

- $R_{jb}$ , is the Joyner-Boore distance, known as the smallest spacing from the site to the surface projection of the rupture surface;
- $R_{rup}$ , is the shortest distance between the site and the rupture surface;
- $R_{epi}$ , is the distance estimated by the geometric swap.

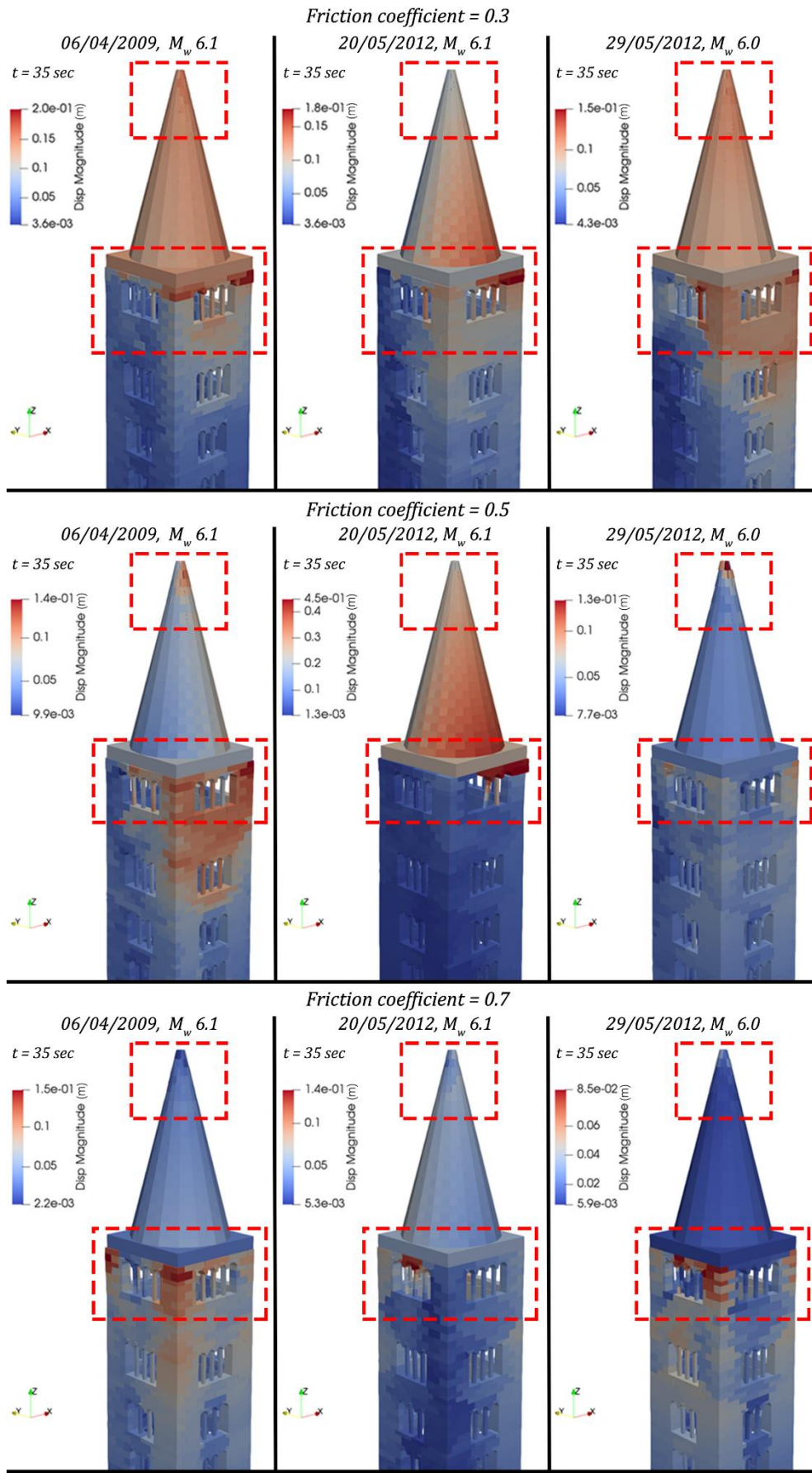
*Table 1\_ Characteristics of main earthquakes recorded in L'Aquila (AQV), Mirandola (MRN), Amatrice (AMT), Campi (CMI), Forca Canapine (FCC) stations during the main seismic events of the last few decades in Italy, where \* indicates that site classification is not based on a direct  $V_s,30$  measurement.*

Seismic event	$M_L$	Depth (km)	Station	Class EC8	$R_{jb}$ [km]	$R_{rup}$ [km]	$R_{epi}$ [km]	Channel NS PGA (cm/s <sup>2</sup> )	Channel EW PGA (cm/s <sup>2</sup> )	Channel UD PGA (cm/s <sup>2</sup> )
06/04/2009	5.9	8.3	AQV	B*	0	5.43	4.90	-535.20	644.25	486.65
20/05/2012	5.9	9.5	MRN	C*	4.34	8.97	16.10	-258.79	-257.23	297.30
29/05/2012	5.8	8.1	MRN	C*	0	3.86	4.10	-288.63	-218.58	-840.74
24/08/2016	6.0	8.1	AMT	B*	1.38	4.62	8.50	368.39	-850.80	391.37
26/10/2016	5.9	7.5	CMI	C*	2.53	7.44	7.10	302.56	-638.31	-468.28
30/10/2016	6.1	9.2	FCC	A*	0	5.55	11.00	843.73	-931.14	893.5

## 5. Discussion of the numerical results

The main results relative to the bell tower of Pomposa and its nonlinear dynamic simulations are reported in **Errore. L'origine riferimento non è stata trovata.**a and **Errore. L'origine riferimento non è stata trovata.**b, in which the principal failure configurations at the last step for each of the eighteen seismic analyses at varying of friction coefficient are plotted.





a)

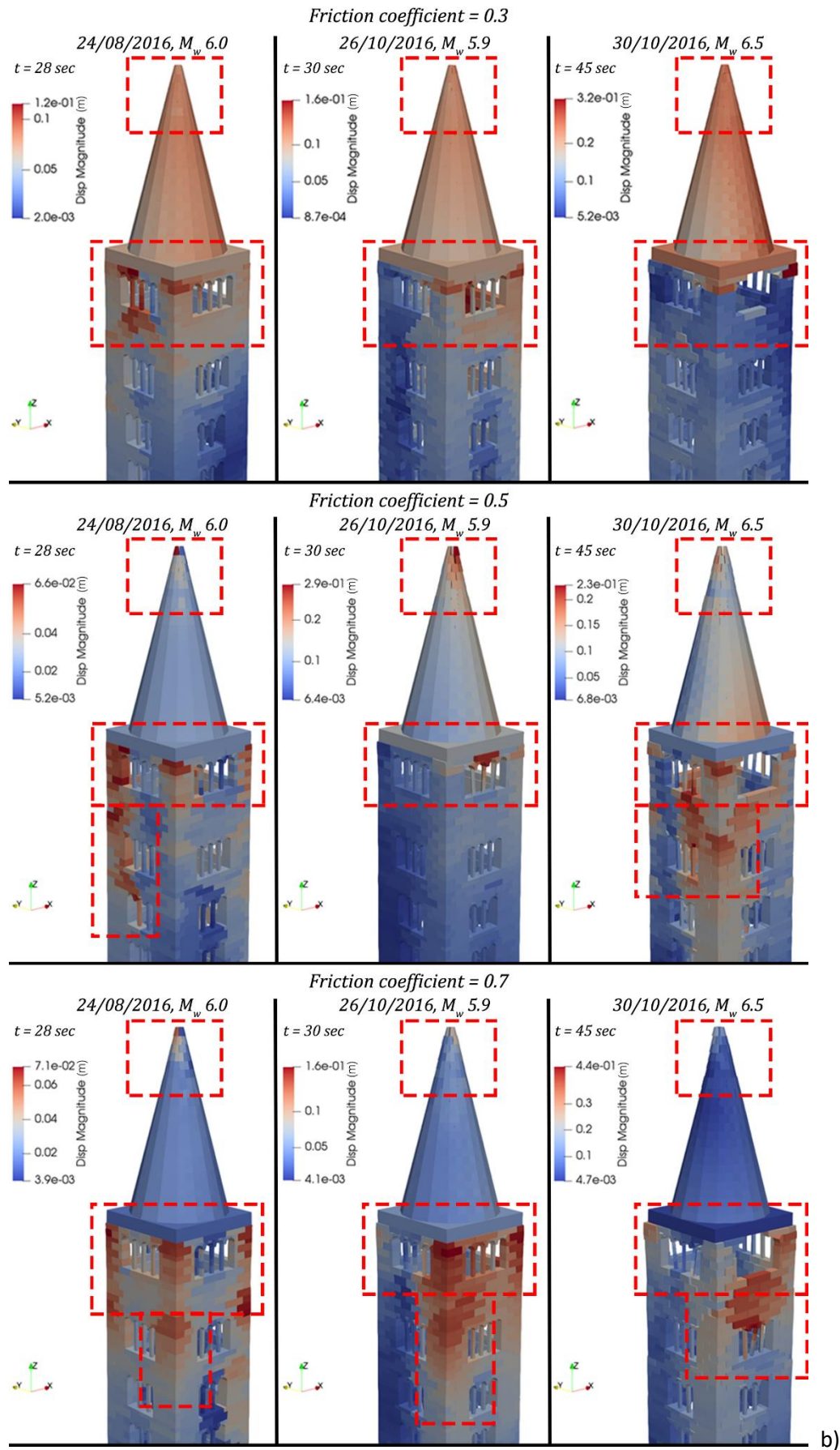


Figure 9\_ Numerical damages of the bell tower of Pomposa Abbey in Codigoro (Italy) under the six main seismic events of the last few decades in Italy at varying of the friction: the L'Aquila and Emilia Romagna (a), the Central Italy (b) earthquakes.

The major damages are revealed at the upper part of the vertical structure and the bell cell for every seismic action applied. As plotted in **Errore. L'origine riferimento non è stata trovata.a** and **Errore. L'origine riferimento non è stata trovata.b**, the principal activated mechanism regarding the rotation of the columns of the arched four-light windows in the bell cell, which engender a typical vulnerability for masonry towers and a partial collapse on the South-West façade under the shocks of 30<sup>th</sup> October 2016 for all values of the friction (see Figure 10).

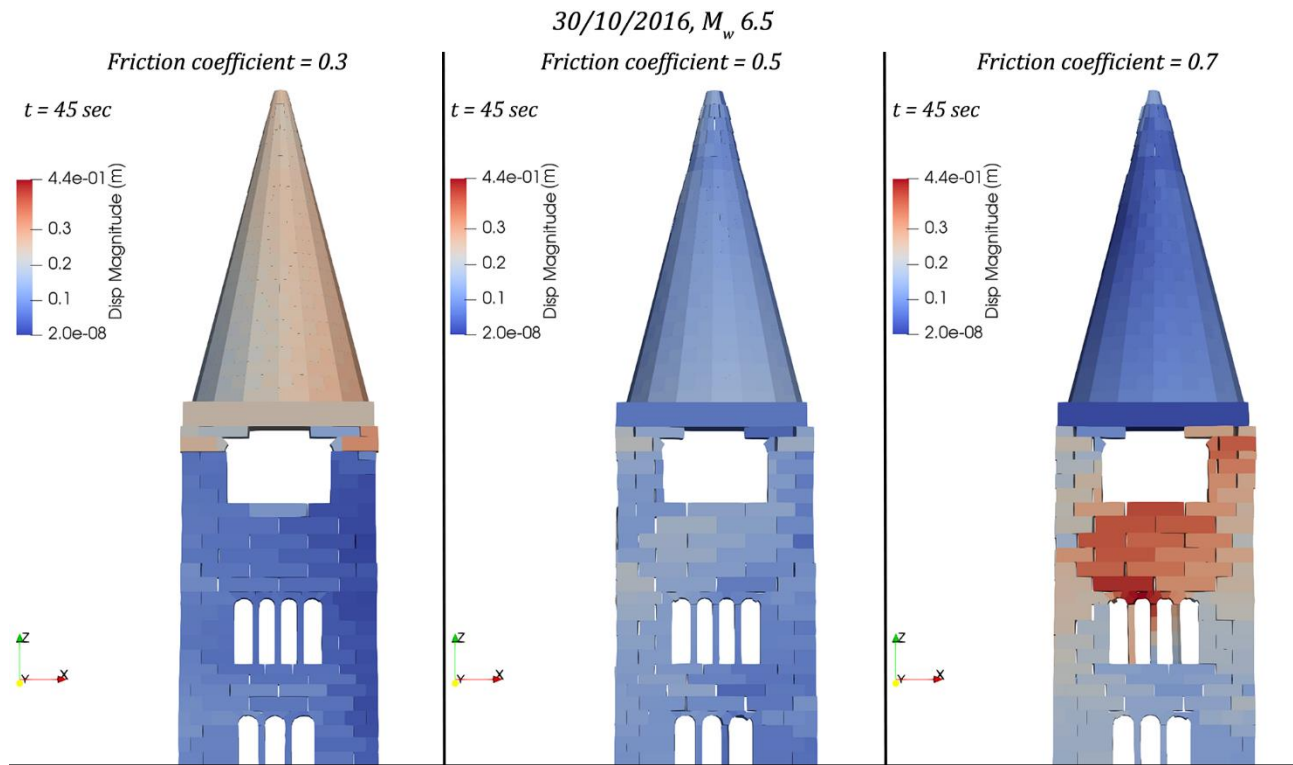


Figure 10\_ Numerical damages of the bell tower of Pomposa Abbey in Codigoro (Italy) under the seismic event of the 30<sup>th</sup> October 2016 in Central Italy at varying of the friction

Along with the longitudinal development of the tower, it is possible to notice the failure mechanisms of the angles highlighted with a red square in **Errore. L'origine riferimento non è stata trovata.a** and **Errore. L'origine riferimento non è stata trovata.b**, only with the friction coefficient equal to 0.5 and 0.7. This collapse mode is evolved more with a higher friction coefficient. In fact, it is not relevant in cases of friction 0.3, then it is observed in two analyses of friction 0.5, with shocks of 24<sup>th</sup> August and 30<sup>th</sup> October 2016, and it is clearly readable in three analyses of friction 0.7, with the three shocks of the seismic sequence of Central Italy of 2016.

In fact, with the increasing of the value of the friction coefficient it is observable that -in general- translation-like mechanisms are substituted with rotation-like mechanisms (see Figure 12). Furthermore, the structure will present many sliding surfaces for small values of the friction coefficient, and as  $\mu$  increases, it is possible to note a clear activation of rotation-like mechanisms of the peripheral walls instead, which leads to major displacements and most localized damage along with the tower. Otherwise, in the presence of a low friction coefficient, there is a pure shear sliding at the base and the formation of a horizontal crack at the base of the tower is clearly visible, which will be much less dissipative than the rotation like mechanisms that will be generated due to greater friction coefficients.



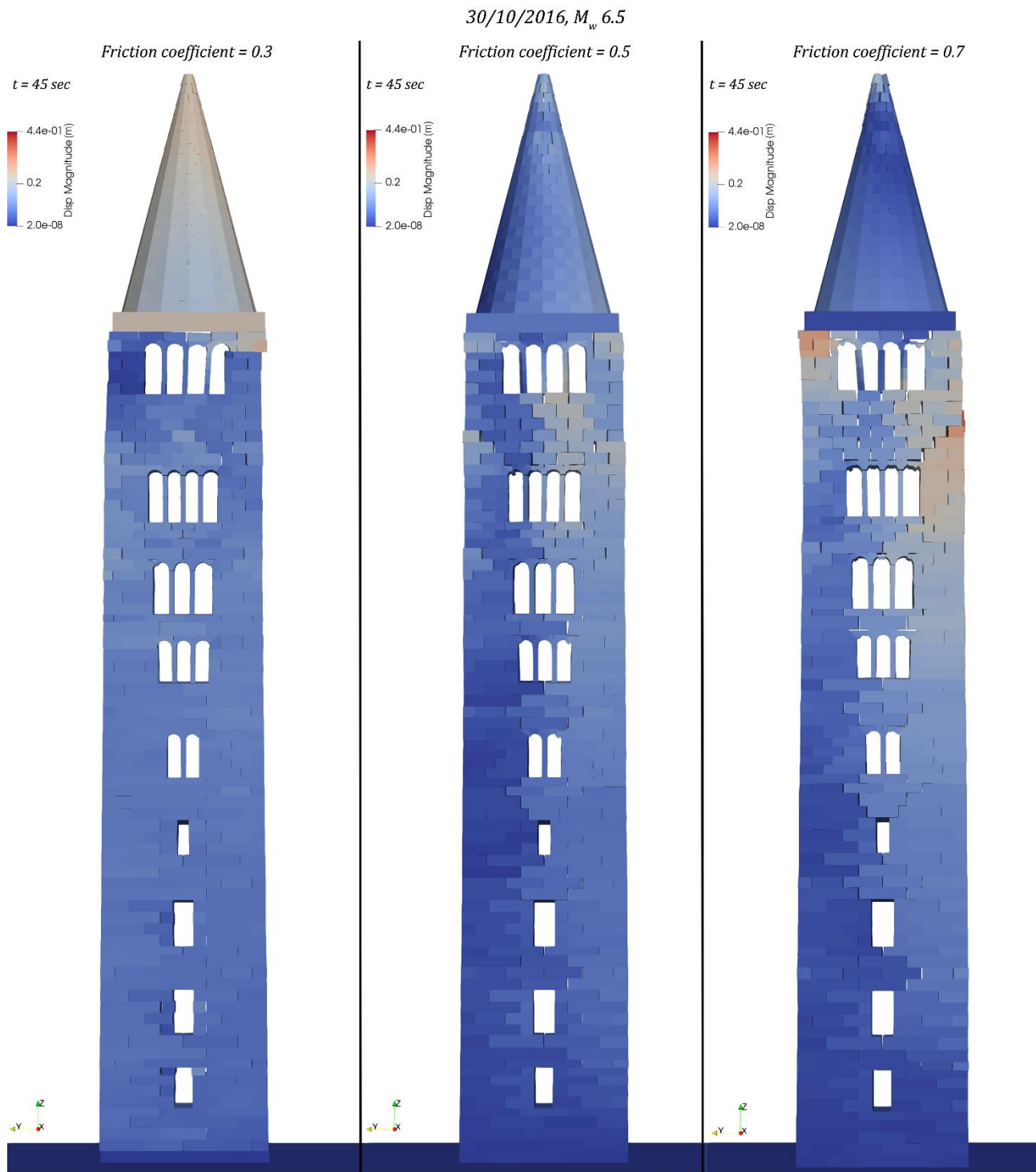
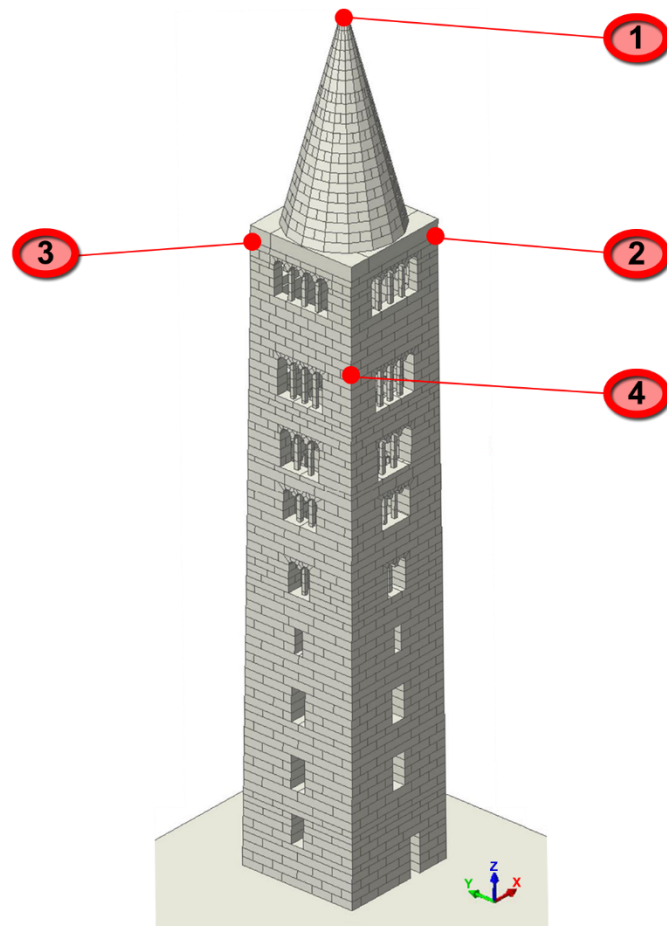


Figure 11\_ Numerical damages of the bell tower of Pomposa Abbey in Codigoro (Italy) under the seismic event of the 30<sup>th</sup> October 2016 in Central Italy at varying of the friction

Another evident activated mechanism is the rotation and the dislocation of the upper part of the conical dome. This damage arises in the results of all the analyses, as highlighted with the red line in **Errore. L'origine riferimento non è stata trovata..** Looking at the outcomes of the event of 30<sup>th</sup> October 2016, it is clear that the upper blocks of the dome have higher displacements and rotations at increasing the value of the friction coefficient.



Control point #1

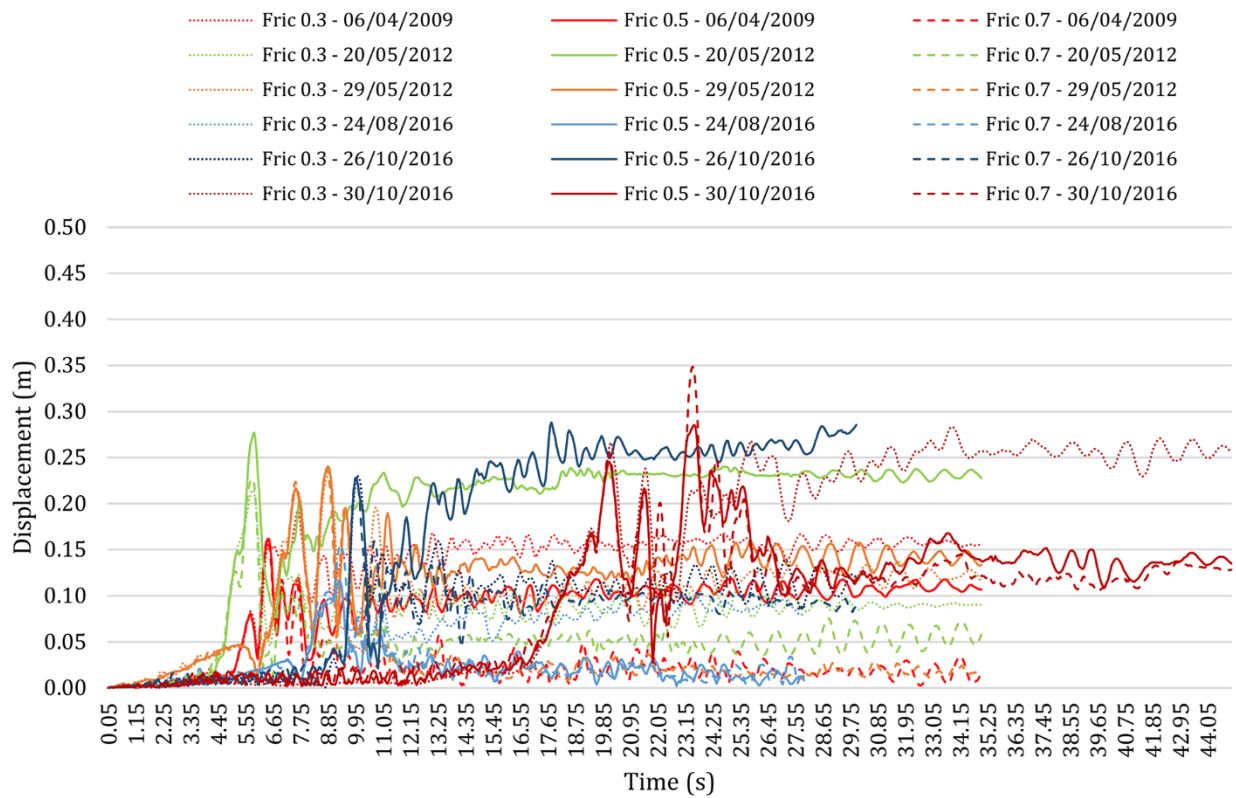


Figure 12\_ Displacements time histories of the control point #1 of the bell tower of Pomposa in Codigoro (Italy) at varying of the friction coefficient under the actions of the six main Italian earthquakes of the last few decades

Additionally, to better understand this last mechanism and to appreciate the amplification of the deformations due to the various friction values, it is necessary to comprehend the displacements of the control point #1 over time plotted in Figure 12, i.e. related to the pinnacle of the dome. In fact, the displacements Time Histories (THs) present the results of the analyses with friction 0.3, using the dotted line, friction 0.5, marked by the solid line, and friction 0.7, with a dashed line.

The resultant displacements of the three models are quite similar for every shock used. The peaks of ~35 cm, for the model with friction 0.7, ~30 cm, for friction 0.5, and ~22 cm, for friction 0.3 relative to the events of 30<sup>th</sup> October 2016, confirm what explained above about the larger dislocations corresponding to rotation-like mechanisms for higher values of the friction coefficient. Moreover, the model with a minor friction value shows residual displacement higher for shocks of 06<sup>th</sup> April 2009, 24<sup>th</sup> August 2016, 30<sup>th</sup> October 2016 mainly due by sliding on blocks of the first courses, close to the base.

Differently, the control points #2 (see Figure 13), at the base of the dome, presents relevant residual dislocations for the models with friction 0.3, equal to 20 cm for the action of 06<sup>th</sup> April 2009, 15 cm for the 29<sup>th</sup> May 2012, 10 cm 24<sup>th</sup> for the August 2016, 31 cm for the 30<sup>th</sup> October 2016. The same motions for the models characterized by friction 0.5 e 0.7 have lesser values of residual displacements. An inverted case concerns the analyses with earthquakes of 20<sup>th</sup> May 2012, in which is higher the dislocation of the model with friction 0.5, that has a residual value equal to 44 cm, than the models with friction 0.3 and 0.7, which have respectively value of 16 cm and 5 cm.

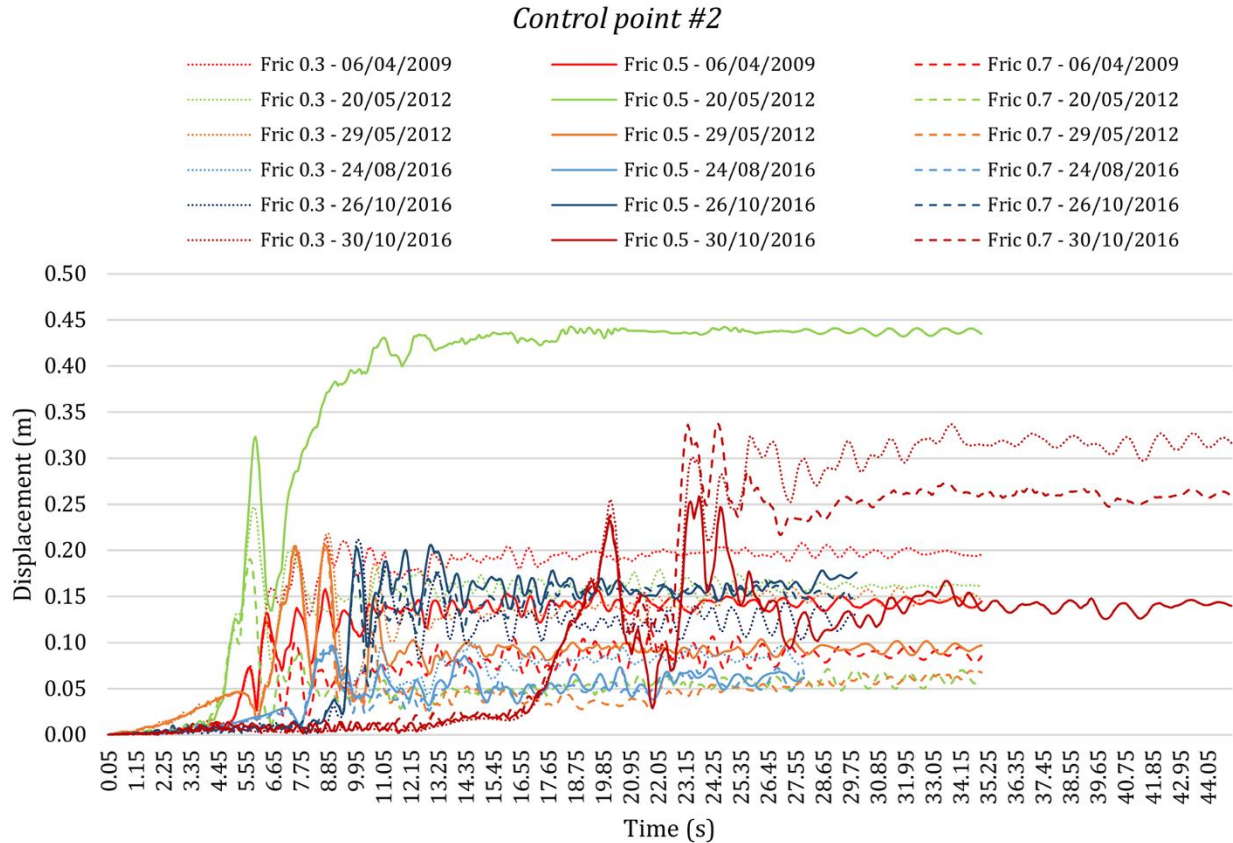


Figure 13\_ Displacements time histories of the control point #2 of the bell tower of Pomposa in Codigoro (Italy) at varying of the friction coefficient under the actions of the six main Italian earthquakes of the last few decades

Looking at the displacements THs of the control point #3 plotted in Figure 14, the peak and the residual values are higher for the models with friction 0.7 than the others with minor friction for every seismic action. Otherwise, the models with friction 0.3 and 0.5 present quite near values of the displacements.

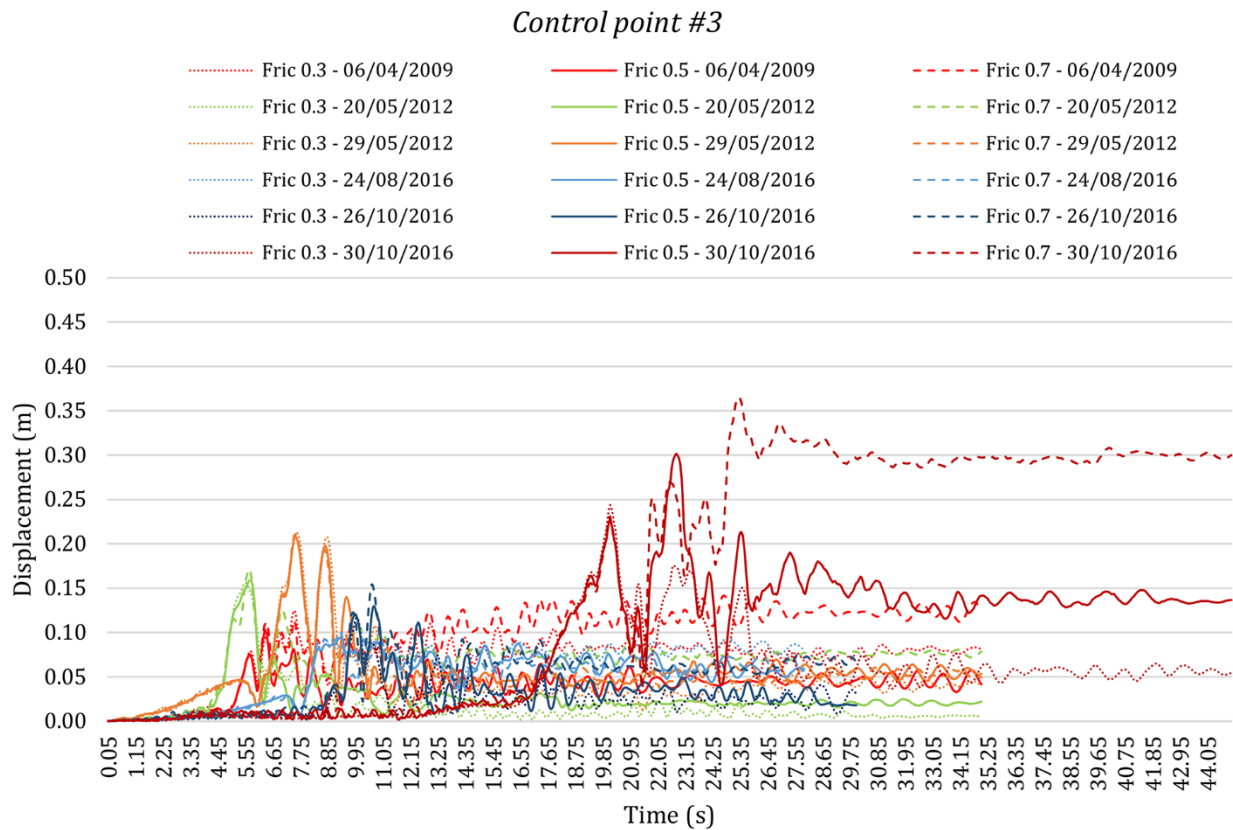


Figure 14\_ Displacements time histories of the control point #3 of the bell tower of Pomposa in Codigoro (Italy) at varying of the friction coefficient under the actions of the six main Italian earthquakes of the last few decades

For what concerns the displacements THs of the control point #4 (see Figure 15), belonging to the elevation of the tower, they present comparable values of displacement with those highlighted in **Errore. L'origine riferimento non è stata trovata.**. In particular, the residual motions related to the 30<sup>th</sup> October 2016 are equal to 25 cm for friction 0.7, 20 cm for friction 0.5 and 10 cm for friction 0.3. Similarly, the residual displacements about the events of 24<sup>th</sup> August 2016 and 26<sup>th</sup> October 2016 present the same behaviours.

When it comes to the vertical development of the tower, it is possible to notice the failure mechanisms along with the development of the angles highlighted with red in **Errore. L'origine riferimento non è stata trovata.**, only about the friction equal to 0.5 e 0.7. This collapse mode is more evolved with a higher friction coefficient. In fact, it is not relevant in the cases of friction 0.3, then it is observed in two analyses of friction 0.5, with shocks of 24<sup>th</sup> August and 30<sup>th</sup> October 2016, and it is clearly readable in three analyses of friction 0.7, with the three shocks of the seismic sequence of Central Italy of 2016.



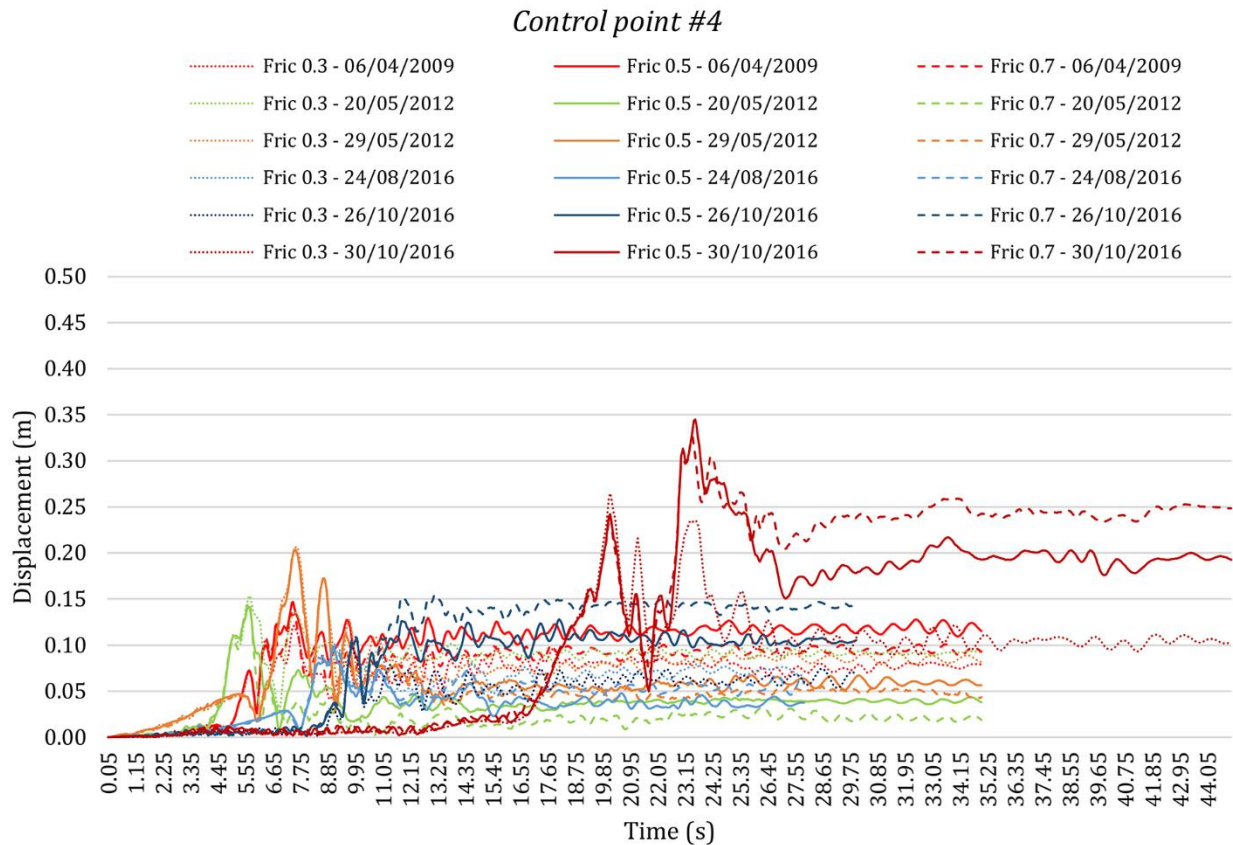


Figure 15\_ Displacements time histories of the control point #4 of the bell tower of Pomposa in Codigoro (Italy) at varying of the friction coefficient under the actions of the six main Italian earthquakes of the last few decades

Lastly, for all the models, the dissipated energy is plotted and reported **Errore. L'origine riferimento non è stata trovata.** in Figure 16 at the varying of the friction coefficient and the shocks used. Thus, in the cases of 6<sup>th</sup> April 2009, 24<sup>th</sup> August 2016, and 30<sup>th</sup> October 2016, the higher values for the dissipation of energy belong to the models with friction 0.7 (indicated with dashed line), with values quite near to those of the models with friction 0.5 (indicated with solid line). Otherwise, for these events, the models with friction 0.3 (indicated with dotted line) have the lowest dissipated energy, even if the difference is not so significant compared to the previous ones. For the case of 26<sup>th</sup> October 2016, the highest energy is due to the friction 0.5, after the friction 0.7 and finally the 0.3. The response of the structures is different to the events of 20<sup>th</sup> and 29<sup>th</sup> May 2012, which present opposite behaviors. In fact, the major dissipated energy depends on the friction 0.3 while minor is due to the friction 0.7.

From the analysis of the dissipated energy (Figure 16) it is also evident that the formation of a horizontal sliding crack at the base of the tower associated with different sliding cracks along the vertical development of the tower can be associated to a reduced dissipation. On the other hand, for masonry with a better mechanical performance, it is possible to highlight a greater ability to form macro-elements that can be involved in the in-plane or out-of-plane rotations.

## Dissipation of Energy

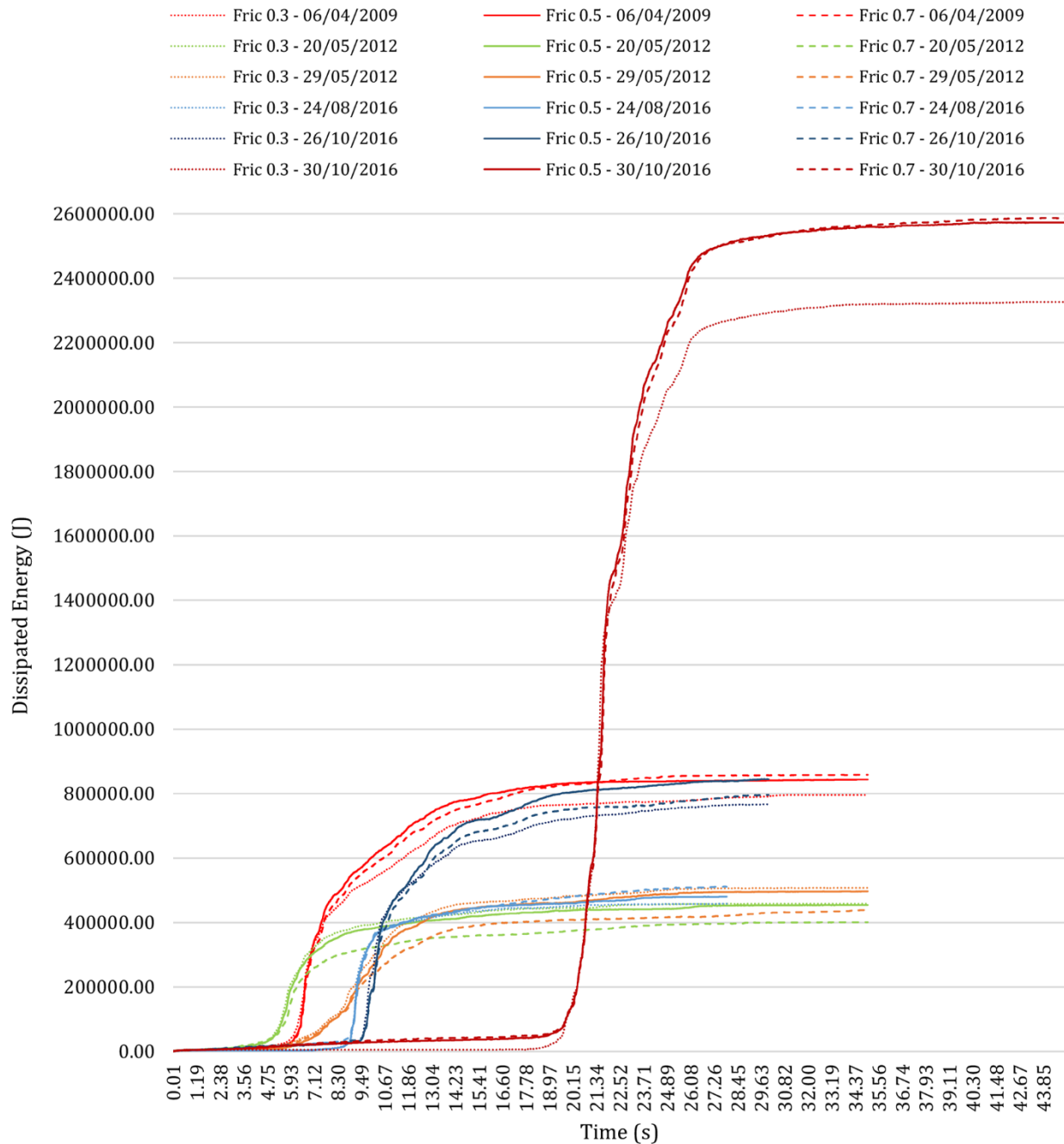


Figure 16\_ Evolution of the dissipated energy of bell tower of Pomposa in Codigoro (Italy) at varying the friction coefficient under the actions of the six main Italian earthquakes of the last few decades

## 6. Conclusions

The results obtained for the bell tower of Pomposa Abbey in Codigoro (Italy), under the six main seismic events of the last few decades in Italy, are here briefly reported and summarized, underlining the failure mechanisms of this type of structure, especially at the upper level, and the incidence of the different possible values that may be attributed to the friction coefficient.

To a complete comprehension of the mechanical response of such complex ancient structures to seismic loading, pointing out the same portions most damaged during the seismic actions, a discontinuous approach and the NSCD method were used, implemented in the LMGC90©. It combines modelling simplicity and great predictive capabilities.

Its ease comes from the following fundamental simplifying assumptions: (i) block rigidity; (ii) simple contact laws between blocks; (iii) absence of any damping. As a result, the mechanical behaviour of the masonry structures is influenced by only the friction coefficient, relative to the existing materials and which assumes the values relative to the current configuration of the analysed bell tower. This is a significant consequence for modelling ancient buildings, since the determination of the mechanical properties of these masonries is always uncertain and variable. Despite its simplicity, the model can predict a large variety of dynamical behaviours of historical structures and their seismic vulnerability. Depending on the values assigned to the friction coefficient, different failure mechanisms may be found. Indeed, in this case study, the values of the friction were varied to represent the actual situation of the masonry walls and other possible configurations. Thus, it was possible to obtain coherent collapse mechanisms and good matching with the real state of the structure, as well as predicting other potential damages by varying of the masonry mechanical properties.

Finally, the sensitivity of the result to the input parameters, a consequence of the model non-smoothness, are pointed out. This feature is also present in real structures. Indeed, small irregularities in buildings (especially ancient buildings) affect the seismic response in a visible way. However, the overall behaviours (failure mechanisms) of the analysed macro-elements only gradually change with parameters. For instance, if the friction coefficient is considered, the overturning mechanisms become gradually prevailing over sliding mechanisms, as the value of the friction coefficient increases. This represents the main outcomes to understand the existing ancient structures.

Another goal of this work is the suggestion of appropriate retrofitting works in the light of NSCD numerical results and highlighting that sensitivity to data is less evident in the standard FEM continuum models and represents a further distinguishing feature of the proposed approach. Moreover, the need of inserting steel chains is very important for medium-high values of friction coefficients as pointing out by the numerical results, and furthermore how important it is to improve the performance of the mortar in order to ensure a non-disintegrating behaviour under the action of sliding associated with medium-low mortar resistance values.

Finally, these results confirm the large potentialities of the NSCD method applied to large-scale masonry structures and lay down the foundations for future works, in which steel chains should be modelled in the masonry panels and provide the effect of a sequence composed by the main shock and several aftershocks, in order to have a better perception of the real damage.

## References

1. Lagomarsino, S., and Podesta', S. (2004) Damage and Vulnerability Assessment of Churches after the 2002 Molise, Italy, Earthquake. *Earthq. Spectra*, **20** (S1), S271–S283.
2. Milani, G. (2013) Lesson learned after the Emilia-Romagna, Italy, 20-29 May 2012 earthquakes: A limit analysis insight on three masonry churches. *Eng. Fail. Anal.*, **34**, 761–778.

3. Brandonisio, G., Lucibello, G., Mele, E., and Luca, A. De (2013) Damage and performance evaluation of masonry churches in the 2009 L'Aquila earthquake. *Eng. Fail. Anal.*, **34**, 693–714.
4. Valente, M., and Milani, G. (2019) Damage assessment and collapse investigation of three historical masonry palaces under seismic actions. *Eng. Fail. Anal.*, **98**, 10–37.
5. Pellegrini, D., Girardi, M., Lourenço, P.B., Masciotta, M.G., Mendes, N., Padovani, C., and Ramos, L.F. (2018) Modal analysis of historical masonry structures: Linear perturbation and software benchmarking. *Constr. Build. Mater.*, **189**, 1232–1250.
6. Facchini, L., and Betti, M. (2016) Simplified Seismic Analysis of Disordered Masonry Towers. *ASCE-ASME J. Risk Uncertain. Eng. Syst. Part A Civ. Eng.*, **2** (2), C4015010.
7. Facchini, L., and Betti, M. (2017) Time-history analysis of slender masonry towers: a parametric study on the reliability of a simplified Bouc and Wen approach. *Meccanica*, **52** (13), 3181–3196.
8. Bru, D., Ivorra, S., Betti, M., Adam, J.M., and Bartoli, G. (2019) Parametric dynamic interaction assessment between bells and supporting slender masonry tower. *Mech. Syst. Signal Process.*, **129**, 235–249.
9. Bartoli, G., Betti, M., Biagini, P., Borghini, A., Ciavattone, A., Girardi, M., Lancioni, G., Marra, A.M., Ortolani, B., Pintucchi, B., and Salvatori, L. (2017) Epistemic Uncertainties in Structural Modeling: A Blind Benchmark for Seismic Assessment of Slender Masonry Towers. *J. Perform. Constr. Facil.*, **31** (5), 04017067.
10. Bartoli, G., Betti, M., and Monchetti, S. (2017) Seismic Risk Assessment of Historic Masonry Towers: Comparison of Four Case Studies. *J. Perform. Constr. Facil.*, **31** (5), 04017039.
11. Bartoli, G., Betti, M., Marra, A.M., and Monchetti, S. (2019) A Bayesian model updating framework for robust seismic fragility analysis of non-isolated historic masonry towers. *Philos. Trans. R. Soc. A Math. Phys. Eng. Sci.*, **377** (2155), 20190024.
12. Bartoli, G., Betti, M., Galano, L., and Zini, G. (2019) Numerical insights on the seismic risk of confined masonry towers. *Eng. Struct.*, **180**, 713–727.
13. Formisano, A., Vaiano, G., Fabbrocino, F., and Milani, G. (2018) Seismic vulnerability of Italian masonry churches: The case of the Nativity of Blessed Virgin Mary in Stellata of Bondeno. *J. Build. Eng.*, **20**, 179–200.
14. Milani, G., and Valente, M. (2015) Failure analysis of seven masonry churches severely damaged during the 2012 Emilia-Romagna (Italy) earthquake: Non-linear dynamic analyses vs conventional static approaches. *Eng. Fail. Anal.*, **54**, 13–56.
15. Sarhosis, V., Milani, G., Formisano, A., and Fabbrocino, F. (2018) Evaluation of different approaches for the estimation of the seismic vulnerability of masonry towers. *Bull. Earthq. Eng.*, **16** (3), 1511–1545.
16. Monni, F., Clementi, F., Quagliarini, E., Giordano, E., and Lenci, S. (2017) Seismic Assessment of Cultural Heritage: Nonlinear 3d Analyses of “Santa Maria Della Carità” in Ascoli Piceno. *Proc. 6th Int. Conf. Comput. Methods Struct. Dyn. Earthq. Eng. (COMPDYN 2017)*, 2533–2541.
17. Clementi, F., Nespeca, A., and Lenci, S. (2016) Seismic behavior of an Italian Renaissance Sanctuary: Damage assessment by numerical modelling. *Int. Conf. Comput. Methods Sci. Eng. 2016, ICCMSE 2016*, 130004.
18. Catinari, F., Pierdicca, A., Clementi, F., and Lenci, S. (2017) Identification and calibration of the structural model of historical masonry building damaged during the 2016 Italian earthquakes: The case study of Palazzo del Podestà in Montelupone. *AIP Conf. Proc.*, **1906**, 090013.



19. Baraldi, D., Reccia, E., and Cecchi, A. (2018) In plane loaded masonry walls: DEM and FEM/DEM models. A critical review. *Meccanica*, **53** (7), 1613–1628.
20. Reccia, E., Leonetti, L., Trovalusci, P., and Cecchi, A. (2018) A MULTISCALE/MULTIDOMAIN MODEL FOR THE FAILURE ANALYSIS OF MASONRY WALLS: A VALIDATION WITH A COMBINED FEM/DEM APPROACH. *Int. J. Multiscale Comput. Eng.*, **16** (4), 325–343.
21. Malena, M., Portioli, F., Gagliardo, R., Tomaselli, G., Cascini, L., and de Felice, G. (2019) Collapse mechanism analysis of historic masonry structures subjected to lateral loads: A comparison between continuous and discrete models. *Comput. Struct.*, **220**, 14–31.
22. Baraldi, D., de Carvalho Bello, C.B., Cecchi, A., Meroi, E., and Reccia, E. (2019) NONLINEAR BEHAVIOR OF MASONRY WALLS: FE, DE, AND FE/DE MODELS. *Compos. Mech. Comput. Appl. An Int. J.*, **10** (3), 253–272.
23. Baraldi, D., and Cecchi, A. (2018) Discrete and continuous models for static and modal analysis of out of plane loaded masonry. *Comput. Struct.*, **207**, 171–186.
24. Smoljanović, H., Živaljić, N., Nikolić, Ž., and Munjiza, A. (2018) Numerical analysis of 3D dry-stone masonry structures by combined finite-discrete element method. *Int. J. Solids Struct.*, **136–137**, 150–167.
25. Cascini, L., Gagliardo, R., and Portioli, F. (2018) LiABlock\_3D: A Software Tool for Collapse Mechanism Analysis of Historic Masonry Structures. *Int. J. Archit. Herit.*, 1–20.
26. Pierdicca, A., Clementi, F., Isidori, D., Concettoni, E., Cristalli, C., and Lenci, S. (2016) Numerical model upgrading of a historical masonry palace monitored with a wireless sensor network. *Int. J. Mason. Res. Innov.*, **1** (1), 74.
27. Beatini, V., Royer-Carfagni, G., and Tasora, A. (2019) A non-smooth-contact-dynamics analysis of Brunelleschi's cupola: an octagonal vault or a circular dome? *Meccanica*, **54** (3), 525–547.
28. Maio, R., Vicente, R., Formisano, A., and Varum, H. (2015) Seismic vulnerability of building aggregates through hybrid and indirect assessment techniques. *Bull. Earthq. Eng.*, **13** (10), 2995–3014.
29. Asteris, P.G., Sarhosis, V., Mohebkhah, A., Plevris, V., Papaloizou, L., Komodromos, P., and Lemos, J. V. (2015) Numerical Modeling of Historic Masonry Structures, in *Handbook of Research on Seismic Assessment and Rehabilitation of Historic Structures* (eds. Asteris, P., and Plevris, V.), IGI Global, Hershey, PA, pp. 213–256.
30. Pantò, B., Cannizzaro, F., Caddemi, S., and Calì, I. (2016) 3D macro-element modelling approach for seismic assessment of historical masonry churches. *Adv. Eng. Softw.*, **97**, 40–59.
31. Moreau, J.J. (1988) Unilateral Contact and Dry Friction in Finite Freedom Dynamics, in *Nonsmooth Mechanics and Applications*, Springer Vienna, Vienna, pp. 1–82.
32. Formisano, A., and Milani, G. (2019) Seismic Vulnerability Analysis and Retrofitting of the SS. Rosario Church Bell Tower in Finale Emilia (Modena, Italy). *Front. Built Environ.*, **5**.
33. Sarhosis, V., Fabbrocino, F., Formisano, A., and Milani, G. (2017) Seismic vulnerability of different in geometry historic masonry towers. *Proc. 6th Int. Conf. Comput. Methods Struct. Dyn. Earthq. Eng. (COMPDYN 2015)*, 2519–2532.
34. Chetouane, B., Dubois, F., Vinches, M., and Bohatier, C. (2005) NSCD discrete element method for modelling masonry structures. *Int. J. Numer. Methods Eng.*, **64** (1), 65–94.
35. Ferrante, A., Clementi, F., and Milani, G. (2019) Dynamic Behavior of an Inclined Existing Masonry Tower in Italy. *Front. Built Environ.*, **5**.

36. Clementi, F., Ferrante, A., Giordano, E., Dubois, F., and Lenci, S. (2019) Damage assessment of ancient masonry churches stroked by the Central Italy earthquakes of 2016 by the non-smooth contact dynamics method. *Bull. Earthq. Eng.*
37. Ferrante, A., Ribilotta, E., Giordano, E., Clementi, F., and Lenci, S. (2019) Advanced Seismic Analyses of "Apennine Churches" Stroked by the Central Italy Earthquakes of 2016 by the Non-Smooth Contact Dynamics Method. *Key Eng. Mater.*, **817**, 309–316.
38. Poiani, M., Gazzani, V., Clementi, F., Milani, G., Valente, M., and Lenci, S. (2018) Iconic crumbling of the clock tower in Amatrice after 2016 central Italy seismic sequence: advanced numerical insight. *Procedia Struct. Integr.*, **11**, 314–321.
39. Gazzani, V., Poiani, M., Clementi, F., Milani, G., and Lenci, S. (2018) Modal parameters identification with environmental tests and advanced numerical analyses for masonry bell towers: a meaningful case study. *Procedia Struct. Integr.*, **11**, 306–313.
40. Lemos, J. V. (2007) Discrete Element Modeling of Masonry Structures. *Int. J. Archit. Herit.*, **1** (2), 190–213.
41. Ribilotta, E., Giordano, E., Ferrante, A., Clementi, F., and Lenci, S. (2019) Tracking Modal Parameter Evolution of Different Cultural Heritage Structure Damaged by Central Italy Earthquake of 2016. *Key Eng. Mater.*, **817**, 334–341.
42. Brownjohn, J.M.W., De Stefano, A., Xu, Y.-L., Wenzel, H., and Aktan, A.E. (2011) Vibration-based monitoring of civil infrastructure: challenges and successes. *J. Civ. Struct. Heal. Monit.*, **1** (3–4), 79–95.
43. Brownjohn, J.M.. (2007) Structural health monitoring of civil infrastructure. *Philos. Trans. R. Soc. A Math. Phys. Eng. Sci.*, **365** (1851), 589–622.
44. Peeters, B., Maeck, J., and Roeck, G. De (2001) Vibration-based damage detection in civil engineering: excitation sources and temperature effects. *Smart Mater. Struct.*, **10** (3), 518–527.
45. Cunha, A.A.M.F., and Caetano, E. (2006) Experimental Modal Analysis of Civil Engineering Structures. *Sound Vib.*, **40** (6).
46. Clementi, F., Pierdicca, A., Milani, G., Gazzani, V., Poiani, M., and Lenci, S. (2018) Numerical model upgrading of ancient bell towers monitored with a wired sensors network. *10th Int. Mason. Conf.*, 1–11.
47. Lourenco, P.B. (1996) *Computational strategies for masonry structures*.
48. Pulatsu, B., Bretas, E.M., and Lourenco, P.B. (2016) Discrete element modeling of masonry structures: Validation and application. *Earthquakes Struct.*, **11** (4), 563–582.
49. Sarhosis, V., and Lemos, J.V. (2018) A detailed micro-modelling approach for the structural analysis of masonry assemblages. *Comput. Struct.*, **206**, 66–81.
50. Ferraioli, M., Miccoli, L., and Abruzzese, D. (2018) Dynamic characterisation of a historic bell-tower using a sensitivity-based technique for model tuning. *J. Civ. Struct. Heal. Monit.*
51. Boscatto, G., Russo, S., Ceravolo, R., and Fragonara, L.Z. (2015) Global Sensitivity-Based Model Updating for Heritage Structures. *Comput. Civ. Infrastruct. Eng.*, **30** (8), 620–635.
52. Mottershead, J.E., Link, M., and Friswell, M.I. (2011) The sensitivity method in finite element model updating: A tutorial. *Mech. Syst. Signal Process.*, **25** (7), 2275–2296.
53. Campolongo, F., Tarantola, S., and Saltelli, A. (2000) Sensitivity Anaysis as an Ingredient of Modeling. *Stat. Sci.*, **15** (4), 377–395.

54. Circolare Ministeriale n. 617 (2009) Cons. Sup. LL. PP., “Istruzioni per l’applicazione delle Nuove Norme Tecniche per le Costruzioni” di cui al decreto ministeriale del 14.01.2008. G.U. del 26.02.2009 n. 47, supplemento ordinario n. 27. (in Italian).
55. Vasconcelos, G., and Lourenço, P.B. (2009) Experimental characterization of stone masonry in shear and compression. *Constr. Build. Mater.*, **23** (11), 3337–3345.
56. Luzi, L., Pacor, F., and Puglia, R. (2017) Italian Accelerometric Archive v 2.3.
57. Luzi, L., Hailemichael, S., Bindi, D., Pacor, F., Mele, F., and Sabetta, F. (2008) ITACA (ITalian ACcelometric Archive): A Web Portal for the Dissemination of Italian Strong-motion Data. *Seismol. Res. Lett.*, **79** (5), 716–722.
58. Pacor, F., Paolucci, R., Luzi, L., Sabetta, F., Spinelli, A., Gorini, A., Nicoletti, M., Marcucci, S., Filippi, L., and Dolce, M. (2011) Overview of the Italian strong motion database ITACA 1.0. *Bull. Earthq. Eng.*, **9** (6), 1723–1739.